Contribution of Active-Site Residues to the Function of Onconase, a Ribonuclease with Antitumoral Activity†

J. Eugene Lee‡ and Ronald T. Raines*,‡,§

Department of Biochemistry and Department of Chemistry, University of Wisconsin—Madison, Madison, Wisconsin 53706

Received July 2, 2003; Revised Manuscript Received August 2, 2003

ABSTRACT: Onconase (ONC), a homologue of ribonuclease A (RNase A), is in clinical trials for the treatment of cancer. ONC possesses a conserved active-site catalytic triad, which is composed of His10, Lys31, and His97. The three-dimensional structure of ONC suggests that two additional residues, Lys9 and an N-terminal lactam formed from a glutamine residue (Pca1), could also contribute to catalysis. To determine the role of Pca1, Lys9, and Lys31 in the function of ONC, site-directed mutagenesis was used to replace each with alanine. Values of k_{cat}/K_M for the variants were determined with a novel fluorogenic substrate, which was designed to match the nucleobase specificity of ONC and gives the highest known k_{cat}/K_M value for the enzyme. The K9A and K31A variants display 10^3-fold lower k_{cat}/K_M values than the wild-type enzyme, and a K9A/K31A double variant suffers a $>10^4$-fold decrease in catalytic activity. In addition, replacing Lys9 or Lys31 eliminates the antitumoral activity of ONC. The side chains of Pca1 and Lys9 form a hydrogen bond in crystalline ONC. Replacing Pca1 with an alanine residue lowers the catalytic activity of ONC by 20-fold. Yet, replacing Pca1 in the K9A variant enzyme does not further reduce catalytic activity, revealing that the function of the N-terminal pyroglutamate residue is to secure Lys9. The thermodynamic cycle derived from k_{cat}/K_M values indicates that the Pca1···Lys9 hydrogen bond contributes 2.0 kcal/mol to the stabilization of the rate-limiting transition state during catalysis. Finally, binding isotherms with a substrate analogue indicate that Lys9 and Lys31 contribute little to substrate binding and that the low intrinsic catalytic activity of ONC originates largely from the low affinity of the enzyme for its substrate. These findings could assist the further development of ONC as a cancer chemotherapeutic.

Ribonuclease A (RNase A; EC 3.1.27.5) was perhaps the most studied enzyme of the 20th century (*1*, *2*). Although RNase A is still a popular model system for enzymologists and protein chemists, much interest in RNase A has shifted to its variants and homologues that have remarkable biological activities (*3*−*6*). For example, several frog homologues of RNase A are endowed with potent antitumoral and antiviral activity. The ability of these ribonucleases to enter cells and cleave cellular RNA leads to apoptosis (*7*, *8*). One of these frog ribonucleases, Onconase (ONC), is in Phase III clinical trials for the treatment of unresectable malignant mesothelioma, an asbestos-related lung cancer (*9*).

ONC is an 11.8-kDa protein from the oocytes and early embryos of the Northern leopard frog, *Rana pipiens* (*10*). Although ONC and RNase A have 30% amino acid sequence identity and a similar three-dimensional structure (*10*, *11*), the ribonucleolytic activity of ONC with known substrates is 10^4- to 10^5-fold lower than that of RNase A. This low ribonucleolytic activity appears to be paradoxical, as the ribonucleolytic activity of ONC is essential for its cytotoxicity, yet RNase A is not cytotoxic (*12*). Apparently, the low catalytic activity of ONC is offset by other attributes (*13*), including its ability to evade the cytosolic ribonuclease inhibitor protein (RI) (*12*, *14*) and its extraordinary conformational stability ($T_m = 87$ °C) (*15*, *16*).

The active site of ONC lies in the cleft of its kidney shape (*11*). This active site contains the catalytic triad that is characteristic of the RNase A superfamily, preserved as His10, Lys31, and His97 in ONC (cf. His12, Lys41, and His119 in RNase A (*17*)). Two other residues, Pca1 and Lys9, are conserved in the active sites of frog but not mammalian ribonucleases (*18*, *19*). The N-terminal pyroglutamic acid (Pca or <E) of ONC is an uncommon residue found in a variety of proteins and hormones (*20*−*22*), including human RNase 4 and RNase 5 (i.e., angiogenin). A pyroglutamate residue is a lactam formed by the spontaneous or enzyme-catalyzed cyclization of an N-terminal glutamine with the loss of ammonia (*22*, *23*). In crystalline ONC, Pca1 and Lys9 are linked by a hydrogen bond (Figure 1).

† This work was supported by Grant CA73808 (NIH). CD spectroscopy and mass spectrometry were performed at the University of Wisconsin—Madison Biophysics Instrumentation Facility, which was supported by the University of Wisconsin—Madison and Grants BIR-9512577 (NSF) and S10 RR13790 (NIH).

* To whom correspondence should be addressed at the Department of Biochemistry, University of Wisconsin—Madison, 433 Babcock Drive, Madison, WI 53706-1544. Telephone: (608) 262-8588. Fax: (608) 262-3453. E-mail: raines@biochem.wisc.edu.

‡ Department of Biochemistry.

§ Department of Chemistry.

[1] Abbreviations: CD, circular dichroism; <E, pyroglutamic acid; 6-FAM, 6-carboxyfluorescein; MALDI-TOF, matrix-assisted laser desorption ionization−time-of-flight; MES, 2-(*N*-morpholino)ethanesulfonic acid; ONC, Onconase; Pca, pyroglutamic acid; PBS, phosphate-buffered saline; PDB, protein data bank; RI, ribonuclease inhibitor protein; rmsd, root-mean-square deviation; RNase A, ribonuclease A; 6-TAMRA, 6-carboxytetramethylrhodamine.

10.1021/bi035147s CCC: $25.00
Published on Web 09/12/2003

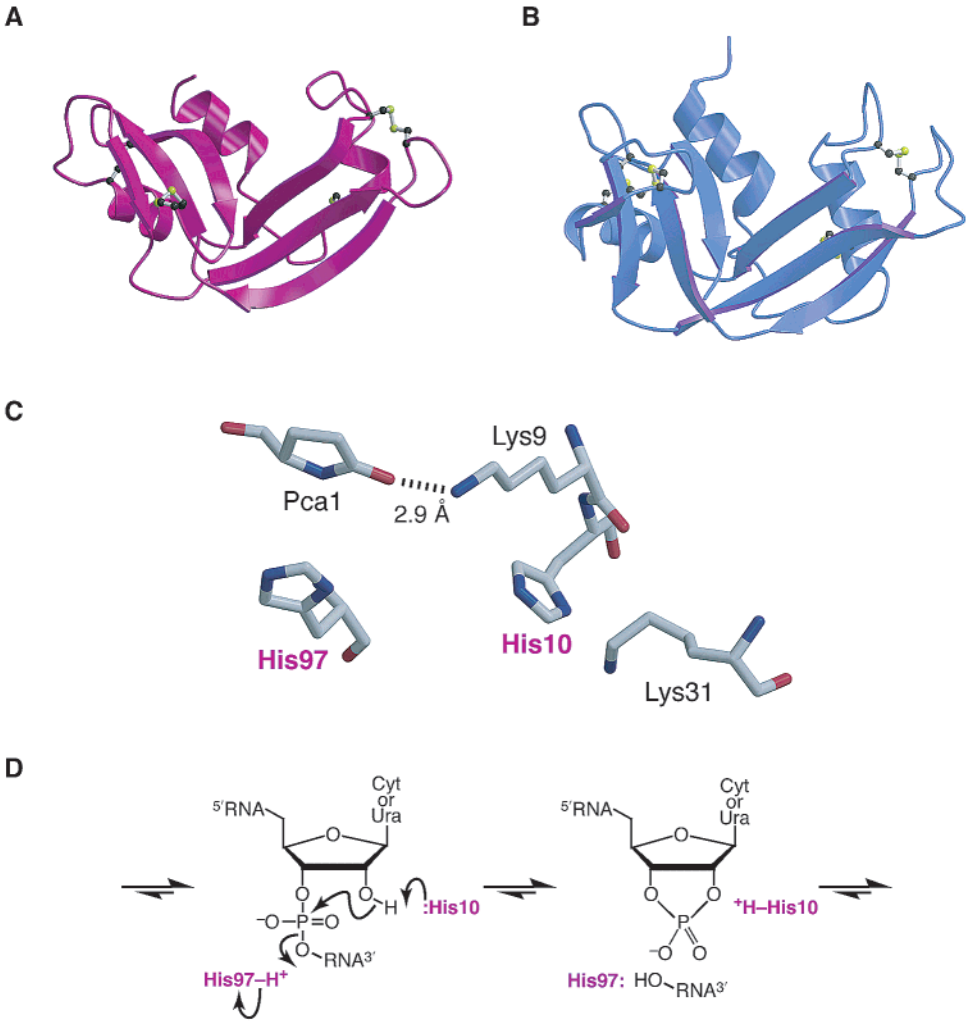

FIGURE 1: Structure and function of Onconase. (A) Three-dimensional structure of ONC (PDB entry 1ONC (*11*)). (B) Three-dimensional structure of RNase A (PDB entry 7RSA (*24*)), which is a homologue of ONC. (C) Active-site residues of ONC. His10, Lys31, and His97 are conserved in the RNase A superfamily (*18*). Pca1 and Lys9 are absent from RNase A and its mammalian homologues (*19*). Images were created with the program MOLSCRIPT and rendered with the program RASTER3D (*25*). (D) Putative mechanism of catalysis of RNA cleavage by ONC.

Little is known about catalysis by ONC. The few previous studies have employed heterogeneous substrates and variants of ONC having an additional N-terminal methionine residue, which lies near the active site and precludes the cyclization of Gln1 to form Pca1 (*26*, *27*). Here, we have produced active-site variants of ONC without any additional residues at the N-terminus. We have also developed a novel homogeneous substrate for ONC that has allowed us to measure kinetic parameters accurately, even for ONC variants of low catalytic activity. We use these tools to address the following mechanistic issues: (1) How do the active-site lysine residues of ONC contribute to transition-state and ground-state binding? (2) What is the role in catalysis of the hydrogen bond between Pca1 and Lys9? (3) What is the origin of the low ribonucleolytic activity of ONC?

EXPERIMENTAL PROCEDURES

Materials. Human RI (as RNasin) was from Promega (Madison, WI). 6-Carboxyfluorescein-dArUdAdA-6-carboxytetramethylrhodamine (6-FAM-dArUdAdA-6-TAMRA), 6-FAM-dArUdGdA-6-TAMRA, and 6-FAM-dAdUdGdA were from Integrated DNA Technology (Coralville, IA). 2-(*N*-Morpholino)ethanesulfonic acid (MES) was from Sigma Chemical (St. Louis, MO). MES was purified further by anion-exchange chromatography prior to its use so as to eliminate oligo(vinylsulfonic acid), which is a potent inhibitor of ribonucleases (*28*). [methyl-^3H]Thymidine was from PerkinElmer Life Sciences (Boston, MA). Phosphate-buffered saline (PBS) contained (in 1 L) 0.20 g of KCl, 0.20 g of KH_2PO_4, 8.0 g of NaCl, and 2.16 g of $Na_2HPO_4 \cdot 7H_2O$. All other chemicals and reagents were of commercial grade or better and were used without further purification.

K-562 cells, which derive from a continuous human chronic myelogenous leukemia line, were from the American Type Culture Collection (Manassas, VA). The cell culture medium and supplements were from Invitrogen (Carlsbad, CA).

Instruments. Mass was measured by matrix-assisted laser desorption ionization−time-of-flight (MALDI-TOF) mass spectrometry using a Voyager-DE-PRO Biospectrometry Workstation (Applied Biosystems, Foster City, CA) and a 3,5-dimethoxy-4-hydroxycinnamic acid (sinapinic acid) matrix (Sigma Chemical). Fluorescence measurements were performed with a QuantaMaster 1 photon counting fluorometer equipped with sample stirring (Photon Technology

International, South Brunswick, NJ). Fluorescence anisotropy measurements were made with a Beacon 2000 fluorescence polarization system (Panvera, Madison, WI). Circular dichroism (CD) experiments were performed with a model 62A DS CD spectrophotometer (Aviv, Lakewood, NJ) equipped with a temperature controller. Radioactivity was quantitated with a Microbeta TriLux liquid scintillation and luminescence counter (PerkinElmer, Wellesley, MA).

Production of ONC and Its Variants. Wild-type ONC was produced in *E. coli* with pONC, a pET-22b(+)-based vector described previously (*29*). DNA encoding variants of ONC were made from pONC with the QuikChange site-directed mutagenesis kit from Stratagene (La Jolla, CA). All vectors encoded a *pel*B leader sequence at the 5′ end of the ONC coding sequence. The *pel*B leader sequence directs proteins to the periplasmic membrane of *E. coli*, where the sequence is removed by *pelB* peptidase. This expression system enabled us to produce enzymes without any additional amino acids at the N-terminus. Wild-type ONC and its variants were folded oxidatively and purified as described previously (*29*).

Assays of Ribonucleolytic Activity. Ribonucleolytic activity was measured with a hypersensitive assay based on the cessation of fluorescence quenching (*30*). Briefly, the increase of fluorescence at 515 nm was measured upon adding enzyme to 0.020 M MES−NaOH buffer (pH 6.0) containing NaCl (0.010 M), 6-FAM-dArUdGdA-6-TAMRA (50 nM), and human RI (0.1−1.6 nM) at 23 ± 2 °C. The addition of RI eliminates artifacts that could arise from unintentional contamination by RNase A or its human homologue, which bind tightly to RI. Values for k_{cat}/K_M were calculated with the equation

$$k_{cat}/K_M = \left(\frac{(\Delta F/\Delta t)}{F_{max} - F_0}\right)\frac{1}{[E]} \quad (1)$$

In eq 1, $\Delta F/\Delta t$ is the initial slope of the reaction, F_0 is the initial fluorescence intensity, F_{max} is the fluorescence intensity once the reaction is brought to completion, and [E] is the concentration of the enzyme.

Assays of Thermal Stability. CD spectroscopy was used to assess the thermal stability of wild-type ONC and its variants (*15*). A solution of ONC (0.2 mg/mL in PBS) was heated from 25 to 95 °C in 1-°C increments, and the change in molar ellipticity at 204 nm was monitored after a 6-min equilibration at each temperature. CD spectra were fitted to a two-state model for denaturation to determine the value of T_m.

Thermodynamic Cycle. A thermodynamic cycle was constructed from the values of k_{cat}/K_M for the cleavage of 6-FAM-dArUdGdA-6-TAMRA by wild-type ONC and its <E1A, K9A, and <E1A/K9A variants. The effect of a particular mutation on the change in the contribution of free energy ($\Delta\Delta G$) was determined with eq 2:

$$\Delta\Delta G = RT \ln f \quad (2)$$

In eq 2, R is the gas constant, T is temperature in kelvin, and f is the ratio of the k_{cat}/K_M values for the two enzymes being compared (*31*, *32*). The free energy of the interaction between Pca1 and Lys9 ($\Delta\Delta G_{int}$) was calculated with eq 3 (*33*):

$$\Delta\Delta G_{int} = \Delta\Delta G_{wt\rightarrow<E1A/K9A} - \Delta\Delta G_{wt\rightarrow K9A} - \Delta\Delta G_{wt\rightarrow<E1A} \quad (3)$$

Assays of Nucleic Acid Binding. The ability of ONC and its variants to bind to single-stranded DNA was assessed by fluorescence anisotropy (*34*, *35*). All measurements were carried out at 23 ± 2 °C. Protein (∼20 mg) was dissolved in 190 μL of 0.020 M MES−NaOH buffer (pH 6.0) containing NaCl (0.010 M). Half of the protein solution was mixed 1:1 with buffer solution in a new test tube. Serial dilutions were made so as to prepare protein solutions with a wide range of concentrations. 6-FAM-dAdUdGdA (5 μL of a 20 nM solution) was added to each dilution. After 30 min, the fluorescence anisotropy at 520 nm was measured. Anisotropy (A) was defined by the equation

$$A = \frac{I_{||} - I_{\perp}}{I_{||} + 2I_{\perp}} \quad (4)$$

In eq 4, $I_{||}$ and $I_{\perp}$ are the emission components that are parallel and perpendicular to the polarized excitation, respectively. Values of the equilibrium dissociation constant (K_d) were obtained by fitting the anisotropy values at each protein concentration to eq 5, which describes the binding of 6-FAM-dAdUdGdA to a single site on a ribonuclease:

$$A = \frac{(\Delta A)[\text{protein}]}{K_d + [\text{protein}]} + A_{min} \quad (5)$$

Values of K_d were obtained by a nonlinear least-squares analysis, using the program DELTAGRAPH 4.0 (DeltaPoint, Monterey, CA).

Assays of Cytotoxic Activity. The effect of ONC, its variants, and RNase A on cell proliferation was determined by measuring the incorporation of [methyl-^{3}H]thymidine into cellular DNA (*13*−*15*). K-562 cells were grown in RPMI 1640 medium (*36*) containing fetal bovine serum (10% v/v), penicillin (100 units/mL), and streptomycin (100 μg/mL). Cytotoxicity studies were performed using asynchronous log-phase cultures grown at 37 °C in a humidified incubator containing CO_2(g) (5% v/v). To assay toxicity, cells (95 μL of a solution of 5×10^4 cells/mL) were incubated with a 5-μL solution of a ribonuclease or PBS in the wells of a 96-well plate. Cells were then grown for 44 h. Cell proliferation was monitored with a 4-h pulse of [methyl-^{3}H]-thymidine (0.25 μCi/well). Cells were harvested onto glass fiber filters using a PHD cell harvester (Cambridge Technology, Watertown, MA). Filters were washed with water and dried with methanol, and their ^{3}H content was quantitated with liquid scintillation counting.

RESULTS

Production of ONC and Its Variants. The yields of purified ONC and its variants were ≥30 mg per L of culture and comparable to that from a previous study (*15*). Purified proteins appeared as a single band after electrophoresis in a polyacrylamide gel in the presence of sodium dodecyl sulfate (data not shown) and had the expected mass to within 0.05% according to MALDI-TOF mass spectrometry (Table 1).

Development of a Novel Substrate for ONC. Despite ONC sharing a similar three-dimensional structure with RNase A

Table 1: Values of k_{cat}/K_M, m/z, and T_m for ONC and Its Variants

ONC	k_{cat}/K_M[a] (M^{-1} s^{-1})	relative activity (%)	m/z[b] expect.	m/z[b] obsd	T_m[c] (°C)
wild-type	$(1.7 \pm 0.3) \times 10^5$	100	11 820	11 820	85
K9A	$(1.2 \pm 0.1) \times 10^2$	0.071	11 763	11 763	80
K9Q	$(1.7 \pm 0.2) \times 10^2$	0.10	11 820	11 824	>75
K31A	$(1.6 \pm 0.2) \times 10^2$	0.094	11 763	11 767	85
K9A/K31A	$<1.0 \times 10^1$	<0.006	11 706	11 711	78
<E1A	$(7.2 \pm 0.7) \times 10^3$	4.2	11 780	11 783	82
<E1A/K9A	$(1.4 \pm 0.2) \times 10^2$	0.082	11 723	11 727	>75

[a] Values of k_{cat}/K_M are for the cleavage of 6-carboxyfluorescein-dArUdGdA-6-carboxytetramethylrhodamine in 0.020 M MES−NaOH buffer (pH 6.0) containing NaCl (0.010 M) at 23 ± 2 °C. [b] Values of m/z were determined by MALDI-TOF mass spectrometry. [c] Values of T_m were determined in PBS by CD spectroscopy.

(Figure 1), the ribonucleolytic activity of ONC is 10^4- to 10^5-fold lower than that of RNase A using conventional substrates (*26*). The low activity of ONC makes measuring accurate kinetic parameters of low-activity variants problematic. 6-FAM-dArUdAdA-6-TAMRA was designed to match the nucleobase specificity of RNase A and is the best known substrate for RNase A (*30*) and its homologue angiogenin (*37*). This substrate contains a single ribonucleotide embedded within three deoxynucleotides. RNase A and its homologues do not catalyze the cleavage of DNA (*38*, *39*). Hence, 6-FAM-dArUdAdA-6-TAMRA is cleaved by RNase A and angiogenin only between its uridine and adenosine residues.

Unlike RNase A and angiogenin, ONC and other frog ribonuclease homologues prefer to cleave the P−$O^{5'}$ bond of RNA between uridine and guanosine residues (*26*, *40*, *41*). Accordingly, 6-FAM-dArUdGdA-6-TAMRA was designed such that ONC could efficiently cleave the P−$O^{5'}$ bond between the uridine and guanosine residues. This design was successful, as the $k_{cat}/K_M = 2.5 \times 10^4$ M^{-1} s^{-1} value for cleavage of 6-FAM-dArUdGdA-6-TAMRA by wild-type ONC (0.10 M MES−NaOH buffer, pH 6.0, containing 0.10 M NaCl) was at least 10^2-fold greater than that with known substrates (including 6-FAM-dArUdAdA-6-TAMRA) under similar conditions. The use of 6-FAM-dArUdGdA-6-TAMRA enables convenient continuous assays of ONC as well as the acquisition of accurate k_{cat}/K_M values for variants with low ribonucleolytic activity.

Although 6-FAM-dArUdGdA-6-TAMRA is an optimized substrate for ONC, the ribonucleolytic activity of ONC is still much less than that of RNase A. Under the same conditions (0.10 M MES−NaOH buffer, pH 6.0, containing 0.10 M NaCl; 23 ± 2 °C), the value of k_{cat}/K_M for the cleavage of 6-FAM-dArUdGdA-6-TAMRA by ONC is 10^3-fold less than that for the cleavage of 6-FAM-dArUdAdA-6-TAMRA by RNase A (data not shown).

Ribonucleolytic Activity. As listed in Table 1, K9A ONC and K31A ONC were 10^3-fold less active catalysts than wild-type ONC. The K9A/K31A variant did not have any measurable activity, even with 6-FAM-dArUdGdA-6-TAMRA as the substrate ($k_{cat}/K_M < 10$ M^{-1} s^{-1}). Replacing Pca1 with an alanine residue resulted in an enzyme, <E1A ONC, that was 20-fold less active than wild-type ONC. <E1A/K9A ONC had 10^3-fold less activity than the wild-type enzyme.

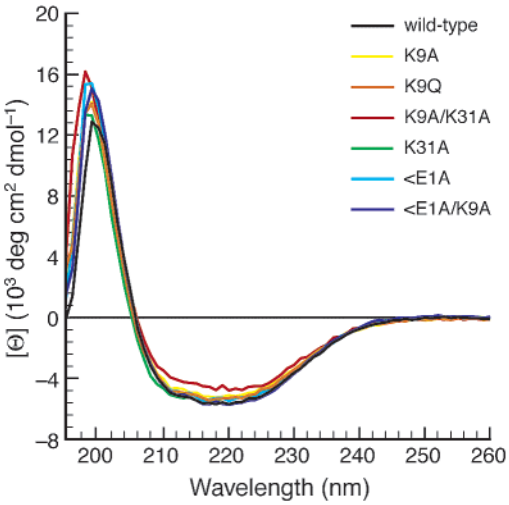

FIGURE 2: Circular dichroism spectra of Onconase and its variants. Spectra are shown as mean residue molar ellipticity ([Θ]) at different wavelengths and were recorded on proteins (0.2 mg/mL) in PBS at 25 °C.

In RNase A, residue 9 is a glutamine rather than a lysine. K9Q ONC was created in an attempt to increase the low ribonucleolytic activity of the wild-type enzyme. The k_{cat}/K_M value of K9Q ONC was, however, 10^3-fold less than that of wild-type ONC (Table 1).

The <E1A/K9A variant of ONC lacks the amino group of Lys9 and has low ribonucleolytic activity. Adding a residue to the N-terminus of this variant could in theory put an amino group in approximately the same position as the missing amino group of Lys9 (cf. Figure 1). The presence of Gly(−1) did not, however, increase the k_{cat}/K_M value of <E1A/K9A ONC (data not shown), suggesting that the α-amino group of Gly(−1) in this variant is not in a position to enhance catalysis.

Thermal Stability. The decrease in the catalytic activity of the ONC variants could be due to a decrease in conformational stability. Accordingly, thermal denaturation studies were performed on each variant. The T_m value of the variants did not decrease by more than 10 °C from that of the wild-type enzyme ($T_m = 85$ °C in PBS). These T_m values (Table 1) along with CD spectra (Figure 2) suggest that the overall structure of each variant is similar to that of wild-type ONC.

Thermodynamic Cycle. Pca1 and Lys9 form a hydrogen bond in crystalline ONC (Figure 1). To discern the free energy of this interaction, the k_{cat}/K_M values for wild-type ONC and its <E1A, K9A, and <E1A/K9A variants were used to construct a thermodynamic cycle for the cleavage of 6-FAM-dArUdGdA-6-TAMRA (Figure 5). The side chain of Lys9 contributes 4.4 kcal/mol to catalysis, whereas that of Pca1 contributes 1.9 kcal/mol. The near zero value of $\Delta\Delta G_{K9A \rightarrow <E1A/K9A} = -0.09$ kcal/mol indicates that Pca1 does not contribute to catalysis if Lys9 is absent from the active site. Finally, the value of $\Delta\Delta G_{int} = -2.0$ kcal/mol reveals that the hydrogen bond between Pca1 and Lys9 stabilizes the rate-limiting transition state during catalysis by 2.0 kcal/mol.

Nucleic Acid Binding. Ribonucleases bind to single-stranded DNA but do not cleave this nucleic acid (*38*, *39*). Hence, binding to single-stranded DNA can be used to assess the affinity of a ribonuclease for its substrate (*34*, *35*).

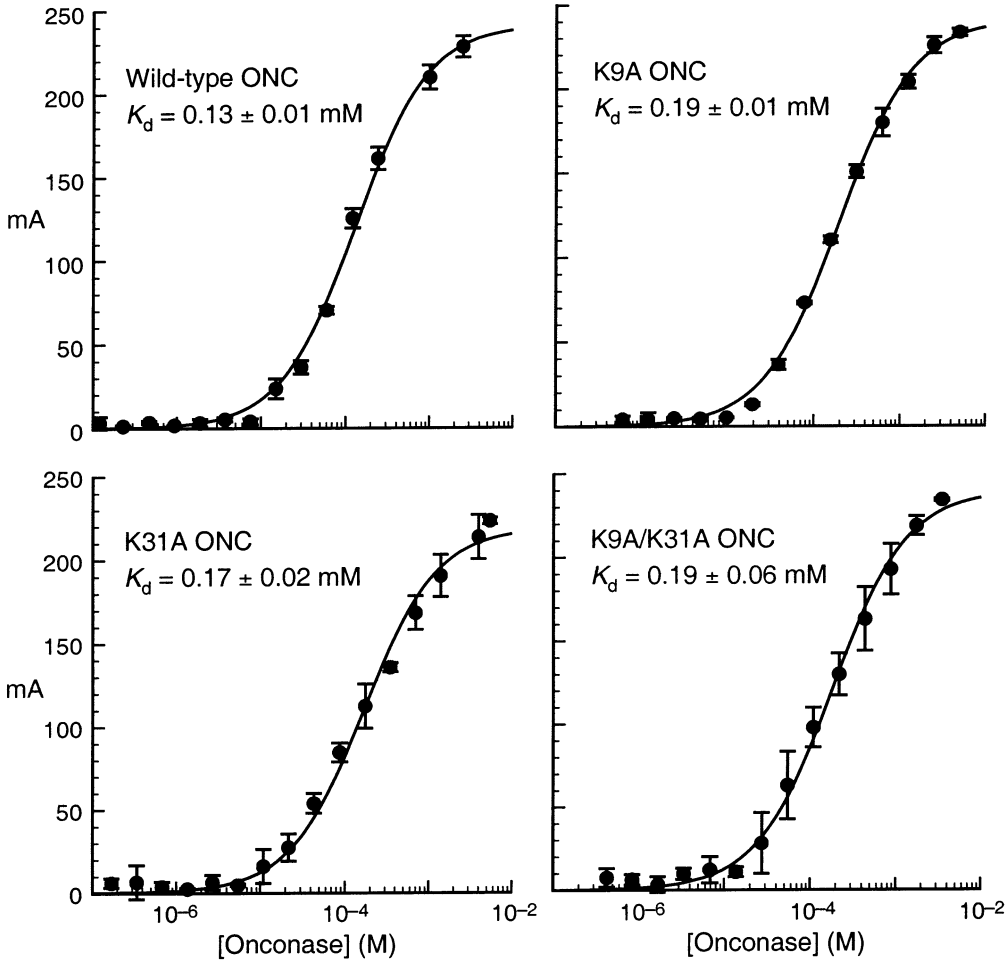

FIGURE 3: Binding isotherms for Onconase and its variants with the ligand 6-FAM-dAdUdGdA. The increase in fluorescence anisotropy was measured in 0.020 M MES−NaOH buffer (pH 6.0) containing NaCl (0.010 M) at 23 ± 2 °C. Values of K_d were obtained by fitting the data points to eq 5 using the program DELTAGRAPH 4.0.

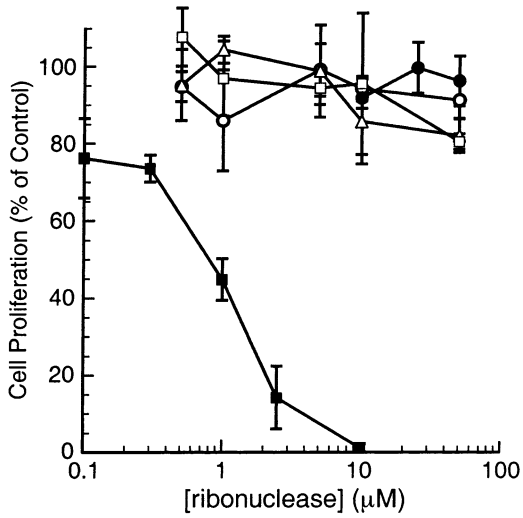

FIGURE 4: Effect of Onconase, its variants, and ribonuclease A on the proliferation of human leukemia cell line K-562. Cell proliferation was determined by incorporation of [methyl-^{3}H]thymidine into cellular DNA after a 44-h incubation with a ribonuclease. Each data point (■, wild-type ONC; ○, K9A ONC; △, K31A ONC; □, K9A/K31A ONC; ●, RNase A) is expressed as a percentage of the PBS control.

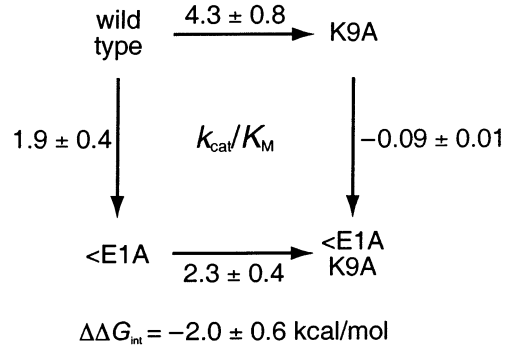

FIGURE 5: Thermodynamic cycle of k_{cat}/K_M for the cleavage of 6-FAM-dArUdGdA-6-TAMRA by Onconase upon replacing Pca1 or Lys9 (or both) with alanine. Values of $\Delta\Delta G$ (in kcal/mol) were calculated with eq 2 and the k_{cat}/K_M values in Table 1. $\Delta\Delta G_{int}$ is the free energy of interaction between the side chains of Pca1 and Lys9, and was calculated with eq 3 and the data in Table 1.

Isotherms for the binding to 6-FAM-dAdUdGdA, which contains the same nucleobases as the 6-FAM-dArUdGdA-6-TAMRA substrate, were obtained by measuring fluorescence anisotropy and are shown in Figure 3. Unexpectedly, these data reveal that replacing Lys9 or Lys31 (or both) with alanine had little effect on the affinity of ONC for a single-stranded nucleic acid, even in a solution of low salt concentration (0.010 M NaCl) that enables the manifestation of Coulombic interactions.

Cytotoxicity Activity. The toxicity of each ribonuclease was measured with the K-562 human leukemia cell line. Wild-type ONC had an IC_{50} value of 0.8 μM (Figure 4), which is

similar to IC_{50} values reported previously (*13*−*15*). Like wild-type RNase A, the K9A, K31A, and K9A/K31A variants of ONC were not cytotoxic at protein concentrations of ≤50 μM.

DISCUSSION

ONC was discovered 15 years ago (*42*). Since then, more effort has been made to understand its biological actions than its enzymology. We believe that further development of ONC as an antitumoral drug would benefit from a detailed understanding of its catalysis of RNA cleavage.

The three-dimensional structure of ONC is known (*11*), though not in a complex with a nucleic acid. We have used its well-studied homolog, RNase A, as a guide for important active-site residues (*1*, *2*). Although ONC and RNase A possess only 30% amino acid sequence identity, their overall three-dimensional structures are remarkably similar (Figure 1; C^{α} rmsd = 1.7 Å (*43*)). A structural comparison of ONC and RNase A indicates that the active site of ONC is most likely composed of His10, Lys31, and His97, which are conserved within the RNase A superfamily, and Pca1 and Lys9, which are conserved among frog homologues (*18*, *19*). ONC residues His10 and His97 correspond to RNase A residues His12 and His119, which function as the base and acid in catalysis of RNA cleavage (*44*, *45*) and contribute to nucleic acid binding (*35*). Chemical modification of His10 and His97 of ONC showed that these residues are likewise critical for catalysis (*12*). In contrast, the role of the other three active-site residues of ONC is less clear. To elucidate that role, we made variants of ONC in which Pca1, Lys9, and Lys31 are replaced with an alanine residue.

A problem that arises in the study of enyzmes of low intrinsic catalytic activity, such as ONC, is assay sensitivity. To determine accurate kinetic parameters for active-site variants of ONC, a new substrate was necessary. Previous work had shown that frog ribonucleases prefer to cleave RNA between uridine and guanosine residues (*26*, *40*, *41*). Our new substrate, 6-FAM-dArUdGdA-6-TAMRA, is cleaved at least 10^2-fold faster by ONC than any substrate described previously. By using 6-FAM-dArUdGdA-6-TAMRA, we were able to obtain kinetic parameters for low-activity variants.

Role of Lysine Residues in Catalysis. The side chain of Lys41 in RNase A is known to enhance catalysis by forming a hydrogen bond with a nonbridging phosphoryl oxygen during catalysis (*46*, *47*). The corresponding residue in ONC, Lys31, could play a similar role. Interestingly, ONC contains an additional lysine residue in its active-site, Lys9. Most frog ribonucleases have a lysine residue at this position, whereas other RNase A homologues have a conserved glutamine residue (*18*, *19*). Replacing this glutamine residue in RNase A with alanine decreases k_{cat} and K_M but does not affect k_{cat}/K_M, indicating that the glutamine residue contributes to catalysis by promoting the productive binding of a substrate (*48*). To illuminate the role of Lys9 and Lys31 of ONC, we replaced these two lysine residues with alanine. Table 1 shows that replacing either Lys9 or Lys31 with an alanine residue decreases the value of k_{cat}/K_M by 10^3-fold. The catalytic activity of the K9A/K31A double variant was below the sensitivity limit of the assay ($k_{cat}/K_M < 10\ M^{-1}\ s^{-1}$). Thus, in ONC, *two* lysine residues, instead of the single lysine residue in RNase A, are critical for catalysis. From the overall decrease in the k_{cat}/K_M value of the K9A/K31A variant, we conclude that Lys9 together with Lys31 stabilize the rate-limiting transition state by ≥5.9 kcal/mol. We tried to increase the intrinsically low catalytic activity of ONC by replacing a residue of ONC with one from RNase A. Specifically, we replaced Lys9 with glutamine, only to obtain an enzyme with 10^3-fold lower k_{cat}/K_M than wild-type ONC (Table 1). Apparently, the role of Lys9 in ONC differs from that of Gln11 in RNase A.

Single-stranded DNA can bind to a ribonuclease but is not hydrolyzed by the enzyme, enabling binding constants to be obtained without catalytic turnover (*34*, *35*). In RNase A, the K_d value acquired by this method does not differ significantly from the K_M value for analogous substrates (*34*). To facilitate comparisons, we made use of a DNA ligand that has the same nucleobase sequence as the 6-FAM-dArUdGdA-6-TAMRA substrate. The results were surprising (Figure 3). Deleting positive charges in the active site did not have a major effect on nucleic acid binding by the enzyme. The K_d values of the variants are all within 2-fold of that of wild-type ONC. We conclude that the primary function of the two lysine residues in catalysis is to accelerate substrate turnover rather than to enhance substrate affinity. Another interesting aspect of the binding data is the unusually high K_d value of the enzyme·nucleic acid complexes. Indeed, we had to adopt a low salt concentration (0.010 M NaCl) for assays of binding and catalysis, as we were not able to measure accurate binding constants otherwise. The value of K_d for an ONC·nucleic acid complex is $>10^2$-fold greater than that of an analogous RNase A·nucleic acid complex under the same conditions (*34*). This discrepancy indicates that the low intrinsic catalytic activity of ONC originates largely from the low affinity of the enzyme for its substrate.

Role of Lysine Residues in Cytotoxicity. ONC is cytotoxic by virtue of its ability to degrade cellular *t*RNA or *r*RNA (*7*). We tested the cytotoxicity of wild-type ONC and its K9A, K31A, and K9A/K31A variants on a leukemia cell line. None of the variants are cytotoxic, even at a protein concentration of 50 μM, whereas wild-type ONC has an IC_{50} value of 0.8 μM (Figure 4). Thus, the loss of catalytic activity corresponds to a loss of the cytotoxicity, as has been reported for cytotoxic ribonucleases (*12*, *13*, *26*, *41*, *49*). The loss of positive charge(s) could, of course, disrupt other attributes that are necessary for cytotoxicity, including binding to the cell surface, uptake into vesicles, and translocation into the cytosol. Regardless, both active-site lysine residues are required for the cytotoxicity of ONC.

Function of Pyroglutamate Residue. An N-terminal pyroglutamate is found in a variety of enzymes and protein hormones. Its side-chain lactam can form by the enzyme-catalyzed or spontaneous cyclization of an N-terminal glutamine residue (*22*, *50*). The chemical mechanism of cyclization likely involves the nucleophilic attack of the α-amino group of glutamine on the amidic carbon of the side chain with the release of ammonia (*51*). In crystalline ONC, the side-chain oxygen of Pca1 forms a hydrogen bond with the side-chain amino group of Lys9 (Figure 1). (Pca1 likewise forms a hydrogen bond with Lys9 in a crystalline ONC homologue from the frog *Rana catesbeiana* (*41*).) An ONC variant having a methionine residue at the −1 position has 10-fold lower catalytic activity than does wild-type ONC

(*26*). This additional methionine residue precludes the cyclization of Gln1 to produce pyroglutamate, as did Gly(−1) installed in our <E1A/K9A ONC (vide supra). Because we found that the side chain of Lys9 provides an important amino group to the active site, we hypothesized that the Pca1···Lys9 hydrogen bond could limit the rotation of the Lys9 side chain and thereby position its amino group properly for catalysis. To test this hypothesis, we replaced Pca1 with an alanine residue to give <E1A ONC. Loss of the Pca1···Lys9 hydrogen bond results in a 20-fold decrease in ribonucleolytic activity (Table 1), which suggests that the acquisition of rotational freedom by Lys9 undermines catalysis. To verify that the decreased activity was caused by the elimination of the hydrogen bond, rather than the deletion of the Pca1 itself, we prepared a double variant, replacing Pca1 and Lys9 with alanine to give <E1A/K9A ONC. Interestingly, <E1A/K9A ONC has the same catalytic activity as does K9A ONC (Table 1), indicating that once Lys9 is eliminated from the active site, Pca1 does not contribute to the catalysis. These data support our hypothesis that the function of Pca1 is to position Lys9 properly for catalysis through the formation of a hydrogen bond (Figure 1), and reveal a mechanistic imperative for having a pyroglutamate residue at the N-terminus of a protein. Finally, the thermodynamic cycle in Figure 5 and its value of $\Delta\Delta G_{int} = -2.0$ kcal/mol reveal that the Pca1···Lys9 hydrogen bond contributes 2.0 kcal/mol to the stabilization of the rate-limiting transition state during catalysis.

Finally, we note another implication of having a pyroglutamate residue at the N-terminus of ONC. Recently, we created a ribonuclease zymogen by linking the N- and C-termini of RNase A with a protease-recognition sequence (thereby obstructing the active site) and generating new N- and C-termini by circular permutation (*52*). The ribonucleolytic activity of the resulting zymogen is manifested upon proteolysis, engendering a "Trojan horse" strategy for the treatment of diseases that rely on the activity of a protease. Pca1 is essential for the cytotoxicity of ONC (*16*, *26*, *27*) and can form only if Gln1 is the N-terminus. Hence, the zymogen strategy cannot be applied to ONC.

Conclusions. We have investigated the function of the active-site residues of ONC, an RNase A homologue and a possible cancer chemotherapeutic from the Northern leopard frog. We developed a novel fluorogenic substrate for the ribonucleolytic activity assay of ONC, which will facilitate future studies of catalysis. We find that Lys9 and Lys31 of ONC are critical for both catalytic and cytotoxic activity. We reveal that the function of a pyroglutamate residue, Pca1, is to form a hydrogen bond that anchors the side chain of Lys9. Finally, we propose that much of the low intrinsic ribonucleolytic activity of ONC arises from the low affinity of the enzyme for a single-stranded nucleic acid.

ACKNOWLEDGMENT

We are grateful to Dr. B.-M. Kim for help in the initial stages of this work. We thank Prof. E. A. Craig, P. Huang, and P. D'Silva for assistance with fluorescence anisotropy, Drs. J. A. Hodges and D. R. McCaslin for assistance with CD spectroscopy, and Dr. B. G. Miller, E. A. Kersteen, Dr. P. A. Leland, and B. D. Smith for contributive discussions.

REFERENCES

1. Cuchillo, C. M., Vilanova, M., and Nogués, M. V. (1997) Pancreatic ribonucleases, in *Ribonucleases: Structures and Functions* (Riordan, J. F., Ed.) pp 271−304, Academic Press, New York.
2. Raines, R. T. (1998) Ribonuclease A, *Chem. Rev. 98*, 1045−1065.
3. Youle, R. J., and D'Alessio, G. (1997) Antitumor RNases, in *Ribonucleases: Structures and Functions* (Riordan, J. F., Ed.) pp 491−514, Academic Press, New York.
4. Leland, P. A., and Raines, R. T. (2001) Cancer chemotherapy—ribonucleases to the rescue, *Chem. Biol. 8*, 405−413.
5. Matousek, J. (2001) Ribonucleases and their antitumor activity, *Comp. Biochem. Physiol. 129C*, 175−191.
6. Makarov, A. A., and Ilinskaya, O. N. (2003) Cytotoxic ribonucleases: Molecular weapons and their targets, *FEBS Lett. 540*, 15−20.
7. Saxena, S. K., Sirdeshmukh, R., Ardelt, W., Mikulski, S. M., Shogen, K., and Youle, R. J. (2002) Entry into cells and selective degradation of tRNAs by a cytotoxic member of the RNase A family, *J. Biol. Chem. 277*, 15142−15146.
8. Haigis, M. C., and Raines, R. T. (2003) Secretory ribonucleases are internalized by a dynamin-independent endocytic pathway, *J. Cell Sci. 116*, 313−324.
9. Mikulski, S. M., Costanzi, J. J., Vogelzang, N. J., McCachren, S., Taub, R. N., Chun, H., Mittelman, A., Panella, T., Puccio, C., Fine, R., and Shogen, K. (2002) Phase II trial of a single weekly intravenous dose of ranpirnase in patients with unresectable malignant mesothelioma, *J. Clin. Oncol. 20*, 274−281.
10. Ardelt, W., Mikulski, S. M., and Shogen, K. (1991) Amino acid sequence of an anti-tumor protein from *Rana pipiens* oocytes and early embryos, *J. Biol. Chem. 266*, 245−251.
11. Mosimann, S. C., Ardelt, W., and James, M. N. G. (1994) Refined 1.7 Å X-ray crystallographic structure of P-30 protein, an amphibian ribonuclease with anti-tumor activity, *J. Mol. Biol. 236*, 1141−1153.
12. Wu, Y., Mikulski, S. M., Ardelt, W., Rybak, S. M., and Youle, R. J. (1993) A cytotoxic ribonuclease, *J. Biol. Chem. 268*, 10686−10693.
13. Dickson, K. A., Dahlberg, C. L., and Raines, R. T. (2003) Compensating effects on the cytotoxicity of ribonuclease A variants, *Arch. Biochem. Biophys. 415*, 172−177.
14. Haigis, M. C., Kurten, E. L., and Raines, R. T. (2003) Ribonuclease inhibitor as an intracellular sentry, *Nucleic Acids Res. 31*, 1024−1032.
15. Leland, P. A., Staniszewski, K. E., Kim, B.-M., and Raines, R. T. (2000) A synapomorphic disulfide bond is critical for the conformational stability and cytotoxicity of an amphibian ribonuclease, *FEBS Lett. 477*, 203−207.
16. Notomista, E., Catanzano, F., Graziano, G., Gaetano, S. D., Barone, G., and Donato, A. D. (2001) Contribution of chain termini to the conformational stability and biological activity of onconase, *Biochemistry 40*, 9097−9103.
17. Kartha, G., Bello, J., and Harker, D. (1967) Tertiary structure of ribonuclease, *Nature 213*, 862−865.
18. Beintema, J. J., Breukelman, H. J., Carsana, A., and Furia, A. (1997) Evolution of vertebrate ribonucleases: Ribonuclease A superfamily, in *Ribonucleases: Structures and Functions* (Riordan, J. F., Ed.) pp 245−269, Academic Press, New York.
19. Irie, M., Nitta, K., and Nonaka, T. (1998) Biochemistry of frog ribonucleases, *Cell. Mol. Life Sci. 54*, 775−784.
20. Busby, W. H., Quackenbush, G. E., Humm, J., Youngblood, W. W., and Kizer, J. S. (1987) An enzyme(s) that converts glutaminyl-peptides into pyroglutamyl-peptides. Presence in pituitary, brain, adrenal medulla, and lymphocytes, *J. Biol. Chem. 262*, 8532−8536.
21. Fischer, W. H., and Spiess, J. (1987) Identification of a mammalian glutaminyl cyclase converting glutaminyl into pyroglutamyl peptides, *Proc. Natl. Acad. Sci. U.S.A. 84*, 3628−3632.
22. Bateman, R. C., Temple, J. S., Misquitta, S. A., and Booth, R. E. (2001) Evidence for essential histidines in human pituitary glutaminyl cyclase, *Biochemistry 40*, 11246−11250.
23. Lechan, R. M., Wu, P., Jackson, I. M., Wolf, H., Cooperman, S., Mandel, G., and Goodman, R. H. (1986) Thyrotropin-releasing hormone precursor: Characterization in rat brain, *Science 231*, 159−161.
24. Wlodawer, A., Svensson, L. A., Sjölin, L., and Gilliland, G. L. (1988) Structure of phosphate-free ribonuclease A refined at 1.26 Å, *Biochemistry 27*, 2705−2717.

25. Merritt, E. A., and Murphy, M. E. P. (1994) Raster3D Version 2.0, a program for photorealistic molecular graphics, *Acta Crystallogr., Sect. D 50*, 869−873.
26. Boix, E., Wu, Y., Vasandani, V. M., Saxena, S. K., Ardelt, W., Ladner, J., and Youle, R. J. (1996) Role of the N terminus in RNase A homologues: Differences in catalytic activity, ribonuclease inhibitor interaction and cytotoxicity, *J. Mol. Biol. 257*, 992−1007.
27. Newton, D. L., Boque, L., Wlodawer, A., Huang, C. Y., and Rybak, S. M. (1998) Single amino acid substitutions at the N-terminus of a recombinant cytotoxic ribonuclease markedly influence biochemical and biological properties, *Biochemistry 37*, 5173−5183.
28. Smith, B. D., Soellner, M. B., and Raines, R. T. (2003) Potent inhibition of ribonuclease A by oligo(vinylsulfonic acid), *J. Biol. Chem. 278*, 20934−20938.
29. Leland, P. A., Schultz, L. W., Kim, B.-M., and Raines, R. T. (1998) Ribonuclease A variants with potent cytotoxic activity, *Proc. Natl. Acad. Sci. U.S.A. 98*, 10407−10412.
30. Kelemen, B. R., Klink, T. A., Behlke, M. A., Eubanks, S. R., Leland, P. A., and Raines, R. T. (1999) Hypersensitive substrate for ribonucleases, *Nucleic Acids Res. 27*, 3696−3701.
31. delCardayré, S. B., and Raines, R. T. (1995) A residue to residue hydrogen bond mediates the nucleotide specificity of ribonuclease A, *J. Mol. Biol. 252*, 328−336.
32. Radzicka, A., and Wolfenden, R. (1995) Transition state and multisubstrate analog inhibitors, *Methods Enzymol. 249*, 284−312.
33. Mildvan, A. S., Weber, D. J., and Kuliopulos, A. (1992) Quantitative interpretations of double mutations of enzymes, *Arch. Biochem. Biophys. 294*, 327−340.
34. Fisher, B. M., Ha, J.-H., and Raines, R. T. (1998) Coulombic forces in protein-RNA interactions: Binding and cleavage by ribonuclease A and variants at Lys7, Arg10, and Lys66, *Biochemistry 37*, 12121−12132.
35. Park, C., Schultz, L. W., and Raines, R. T. (2001) Contribution of the active site histidine residues of ribonuclease A to nucleic acid binding, *Biochemistry 40*, 4949−4956.
36. Moore, G. E., Gerner, R. E., and Franklin, H. A. (1967) Culture of normal human leukocytes, *J. Am. Med. Assoc. 199*, 519−524.
37. Leland, P. A., Staniszewski, K. E., Park, C., Kelemen, B. R., and Raines, R. T. (2002) The ribonucleolytic activity of angiogenin, *Biochemistry 41*, 1343−1350.
38. Brown, D. M., and Todd, A. R. (1952) Nucleotides. Part X. Some observations on the structure and chemical behaviour of the nucleic acids, *J. Chem. Soc.*, 52−58.
39. Richards, F. M., and Wyckoff, H. W. (1971) Bovine pancreatic ribonuclease, *The Enzymes IV*, 647−806.
40. Okabe, Y., Katayama, N., Iwama, M., Watanabe, H., Ohgi, K., Irie, M., Nitta, K., Kawauchi, H., Takayanagi, Y., Oyama, F., Titani, K., Abe, Y., Oakzaki, T., Inokuchi, N., and Koyama, T. (1991) Comparative base specificity, stability, and lectin activity of two lectins from eggs of *Rana catesbeiana* and *R. japonica* and liver ribonuclease from *R. catesbeiana*, *J. Biochem. (Tokyo) 109*, 786−790.
41. Leu, Y.-J., Chern, S.-S., Wang, S.-C., Hsiao, Y.-Y., Amiraslanov, I., Liaw, Y.-C., and Liao, Y.-D. (2003) Residues involved in the catalysis, base specificity, and cytotoxicity of ribonuclease from *Rana catesbeiana* based upon mutagenesis and X-ray crystallography, *J. Biol. Chem. 278*, 7300−7309.
42. Darzynkiewicz, Z., Carter, S. P., Mikulski, S. M., Ardelt, W. J., and Shogen, K. (1988) Cytostatic and cytotoxic effect of Pannon (P-30 Protein), a novel anticancer agent, *Cell Tissue Kinet. 21*, 169−182.
43. Shindyalov, I. N., and Bourne, P. E. (1998) Protein structure alignment by incremental combinatorial extension (CE) of the optimal path, *Protein Eng. 11*, 739−747.
44. Findlay, D., Herries, D. G., Mathias, A. P., Rabin, B. R., and Ross, C. A. (1961) The active site and mechanism of action of bovine pancreatic ribonuclease, *Nature 190*, 781−784.
45. Thompson, J. E., and Raines, R. T. (1994) Value of general acid−base catalysis to ribonuclease A, *J. Am. Chem. Soc. 116*, 5467−5468.
46. Messmore, J. M., Fuchs, D. N., and Raines, R. T. (1995) Ribonuclease A: Revealing structure−function relationships with semisynthesis, *J. Am. Chem. Soc. 117*, 8057−8060.
47. Messmore, J. M., and Raines, R. T. (2000) Pentavalent organovanadates as transition state analogues for phosphoryl transfer reactions, *J. Am. Chem. Soc. 122*, 9911−9916.
48. delCardayré, S. B., Ribó, M., Yokel, E. M., Quirk, D. J., Rutter, W. J., and Raines, R. T. (1995) Engineering ribonuclease A: Production, purification, and characterization of wild-type enzyme and mutants at Gln11, *Protein Eng. 8*, 261−273.
49. Kim, J.-S., Soucek, J., Matousek, J., and Raines, R. T. (1995) Catalytic activity of bovine seminal ribonuclease is essential for its immunosuppressive and other biological activities, *Biochem. J. 308*, 547−550.
50. Cummins, P. M., and O'Connor, B. (1998) Pyroglutamyl peptidase: An overview of the three known enzymatic forms, *Biochim. Biophys. Acta 1429*, 1−17.
51. Bateman, R. C. (1989) A spectrophotometric assay for glutaminyl-peptide cyclizing enzymes, *J. Neurosci. Methods 30*, 23−28.
52. Plainkum, P., Fuchs, S. M., Wiyakrutta, S., and Raines, R. T. (2003) Creation of a zymogen, *Nat. Struct. Biol. 10*, 115−119.

BI035147S